



Model and Validation of Single-Axis Tracking with Bifacial Photovoltaics

Preprint

Silvana Ayala Pelaez and Raymond K. Kostuk
University of Arizona

Chris Deline
National Renewable Energy Laboratory

Peter Greenberg
NRGWise Lighting

Josh Stein
Sandia National Laboratories

*Presented at the World Conference on
Photovoltaic Energy Conversion (WCPEC-7)
Waikoloa, Hawaii
June 10–15, 2018*

Suggested Citation

Pelaez, S.A., C. Deline, P. Greenberg, J. Stein, and R.K. Kostuk. 2018. "Model and Validation of Single-Axis Tracking with Bifacial Photovoltaics: Preprint." Golden, CO: National Renewable Energy Laboratory. NREL/CP-5K00-72039. <https://www.nrel.gov/docs/fy19osti/72039.pdf>.

**NREL is a national laboratory of the U.S. Department of Energy
Office of Energy Efficiency & Renewable Energy
Operated by the Alliance for Sustainable Energy, LLC**

This report is available at no cost from the National Renewable Energy Laboratory (NREL) at www.nrel.gov/publications.

Conference Paper
NREL/CP-5K00-72039
Revised July 2019

Contract No. DE-AC36-08GO28308

NOTICE

This work was authored by the National Renewable Energy Laboratory, operated by Alliance for Sustainable Energy, LLC, for the U.S. Department of Energy (DOE) under Contract No. DE-AC36-08GO28308. Funding provided by U.S. Department of Energy Office of Energy Efficiency and Renewable Energy Solar Energy Technologies Office. The views expressed in the article do not necessarily represent the views of the DOE or the U.S. Government. The U.S. Government retains and the publisher, by accepting the article for publication, acknowledges that the U.S. Government retains a nonexclusive, paid-up, irrevocable, worldwide license to publish or reproduce the published form of this work, or allow others to do so, for U.S. Government purposes.

This report is available at no cost from the National Renewable Energy Laboratory (NREL) at www.nrel.gov/publications.

U.S. Department of Energy (DOE) reports produced after 1991 and a growing number of pre-1991 documents are available free via www.OSTI.gov.

Cover Photos by Dennis Schroeder: (left to right) NREL 26173, NREL 18302, NREL 19758, NREL 29642, NREL 19795.

NREL prints on paper that contains recycled content.

Errata

This report, originally published online in October 2018, has been revised in July 2019 to update Figure 13b based on revised simulation code Bifacial Radiance v0.3.0 which more accurately locates the rear shading loss position throughout the day. No other findings of the report are affected by this update.

Model and Validation of Single-Axis Tracking with Bifacial PV

Silvana Ayala Pelaez¹, Chris Deline², Peter Greenberg³, Josh Stein⁴, Raymond K. Kostuk¹

¹University of Arizona, Tucson, AZ, 85705, US; ²National Renewable Energy Laboratory, Golden, CO, 80401 US;

³NRGwise Lighting, Albany, OR 97321, US; ⁴Sandia National Laboratories, Albuquerque, NM, 87123, US

Abstract — Single-axis tracking is a cost effective deployment strategy for large-scale ground-mount photovoltaic (PV) systems in regions with high direct-normal irradiance (DNI). Bifacial modules in 1-axis tracking systems boost energy yield by 4% - 15% depending on module type and ground albedo, with a global average of 9%. This benefit is in addition to the 15%-25% energy gain already afforded by single-axis tracking relative to fixed-tilt deployments. Here we compare model results against field performance data for two side-by-side bifacial / monofacial tracked systems – one in Albuquerque NM, and one in eastern Oregon. The Albuquerque system shows monthly rear irradiance gain of 10-14.9%, and the Oregon bifacial system has an average performance ratio 9.4% higher than the monofacial system. Both results match bifacial irradiance model results within uncertainty. Simulations show that smart tracking algorithms can offer more than 1% improvement on annual energy yield by adjusting tilt angle under cloudy conditions. Finally, ray-tracing simulations investigated edge brightening, suggesting 15%-25% increase in rear irradiance at the ends of tracker rows, but up to 20% loss from center-mounted torque tubes, creating multiple shadows.

Index Terms — bifacial PV module, single-axis tracking, irradiance, configuration factor, ray tracing, model, performance.

I. INTRODUCTION

The solar market has seen a renewed interest in bifacial photovoltaic (PV) technology, which promises significant leveled cost of energy savings in comparison to conventional monofacial PV modules [1], [2]. Bifacial solar cells and modules can collect light from both sides including light reflected from the surrounding ground surface. This provides a degree of concentration and is beneficial for space constrained deployments. To some degree the increased output power offsets the higher cost of manufacturing bifacial cells and modules compared to monofacial PV modules. Further cost reduction is expected through large scale manufacturing techniques. Glass-glass modules have also been predicted to have longer operational lifetimes due to better matching of the thermal properties of the package materials [3]. This may also reduce the leveled cost of energy from bifacial modules. Bifacial modules can also be used in one-axis tracking systems to further increase energy yield and offset system cost. Bizarri [4] recently presented results from the La Silla PV plant in Chile, where a 550 kWp single-axis bifacial module array demonstrated a 12% increase in performance with respect to standard single-axis monofacial technology. Stein et al report daily potential bifacial gains between 8%-14% for two single-axis trackers at Albuquerque, New Mexico [5]. This promising result suggests that further evaluation and optimization could lead to significant increases in energy yield for bifacial PV systems in one-axis tracking configurations.

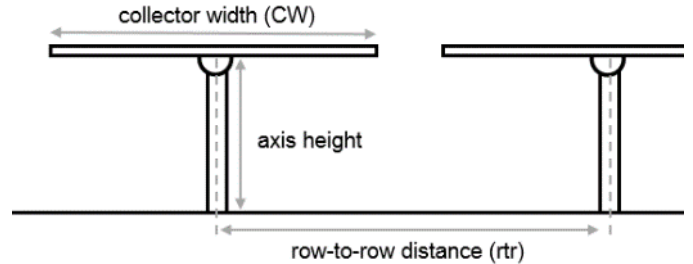


Fig. 1. On a tracking system, the fixed parameters are the distance between the centers of rotation, and the axis height. Module ground clearance, tilt, and separation between arrays varies with the solar position.

In this work, we compare measured field performance of several single-axis tracked bifacial systems with neighboring monofacial systems, and with modeled expectation based on two bifacial irradiance models. In prior work, we described a RADIANCE [6] -based ray trace model and configuration factor (CF) model [7] for rear-side irradiance G_{rear} calculation of fixed-tilt systems, and verified them for fixed-tilt conditions with field data [7]–[9]. Here we extend these models for single-axis tracking applications.

The Radiance model offers the possibility of reproducing complex scenes, including tracker element shading. Run times of several seconds or minutes are possible with simple geometry and when using a cumulative-sky approach which calculates front-side and rear-side bifacial irradiance based on a single annual cumulative sky source for the year [10]. This composite source comprises all hourly Perez diffuse sky and direct solar contributions for the year. The CF model also incorporates the Perez tilted surface model [11], and assumes a 2D geometry to calculate the fractional irradiance entering and leaving the surfaces of an infinite-length PV array. This approach is also fast (~ seconds) but does not include complex shading or finite system edge effects.

Both models are freely downloadable [12], [13] and can be used to evaluate single-axis tracking scenarios. With single-axis tracking, the modules are no longer at a fixed tilt, and the clearances to the ground and with neighboring rows in the array are constantly changing. Tracking algorithms can be used to calculate these parameters, based on the ground coverage ratio (GCR):

$$GCR = \frac{CW}{rtr} \quad (1)$$

where CW is the PV collector width (overall width of the modules in a row), and rtr is the distance between the rotation axis of the

panels as shown in Fig. 1. GCR is used in tracking algorithms to implement backtracking corrections to the tilt of the trackers, based on minimizing shading from neighboring arrays. This correction becomes particularly important for arrays with higher GCRs. We can also define a normalized axis height H :

$$H = \frac{\text{axis height}}{cw} \quad (2)$$

These normalized parameters allow comparisons between tracker designs of different dimension (e.g. 2-up landscape vs 2-up portrait) since the self-shading geometry and bifacial rear irradiance is dependent on these normalized parameters, not on absolute dimensions.

Once the position of the tracker is known, the Perez tilted surface model can be recalculated for each configuration. For the raytrace model, a modified cumulative sky is used to determine the diffuse sky irradiance received by the array at different angles throughout the year.

II. BIFACIAL MODELS FOR 1-AXIS TRACKING

The tracking algorithm from PVLlib [14] is used to compute the array tilt for both the RADIANCE and CF models. Backtracking corrections have been employed to reduce self-shading of the panels throughout the day based on the ground coverage ratio (GCR) of the system.

A. Tracking CF Model

The CF model described in detail elsewhere [7] has been updated to allow for single-axis tracked bifacial systems. Given an array(s) with a specific axis height and orientation, the additional tracking-specific steps of the CF model are:

- Determining the array's tilt, ground clearance and row to row spacing with other arrays based on the specific time, location, and backtracking (optional).
- Identify the ground region that is shaded by the PV arrays under this configuration.
- Determine the irradiance received by the ground by accounting for shading and restricted view of the sky due to the tracker's position.
- Determine the irradiance for the backside of the PV module.

B. Tracking Radiance Ray Trace Model

The Radiance bifacial PV model [11] has also been updated to allow for tracking systems. Additional steps include calculating the array tilt, ground clearance, and row-to-row spacing for each time step. The conventional fixed-tilt simulation workflow uses a single annual sky source to calculate annual average bifacial gain. For a tracked system, multiple scene geometries are required, along with the solar resource corresponding to each tracker tilt angle. Here we create separate simulation and scene geometry for each tracker tilt in 5° increments, along with the cumulative hourly solar resource corresponding to this solar zenith angle.

III. FIELD COMPARISON SYSTEMS AND METHOD

Several bifacial tracking systems were investigated for this study. The first is a small-scale research array at Sandia National Laboratory, and the second is a set of 100kW commercial systems in eastern Oregon.

A. Sandia National Laboratory PV system

This deployment consists of two rows of 1-axis tracked bifacial modules. Reference cell detectors are mounted on the front and back of some of the modules to measure solar illumination. The tracker axis height is 0.5m, and the trackers are spaced from each other with $GCR = 0.28$. The ground albedo for the site was unmeasured but assumed to be 0.25 for aged concrete. The field data are used to validate modeled G_{rear} / G_{front} using the CF model based on site-measured meteorological data.



Fig. 2. Sandia bifacial tracking array with front and rear irradiance sensor shown (center). Two rows with GCR 0.28

B. Eastern Oregon Demo Site

Two commercial tracked systems east of Klamath Falls, OR are within 20 km of each other. One is composed of 100 kW of Silfab 285 bifacial modules in 2-up landscape, adjacent to 100 kW of Trina 300W monofacial modules in 1-up portrait. The second system is composed of 200 kW of Silfab 285 bifacial modules, also in 2-up landscape orientation. Each system utilizes six Chint 36kW inverters, with AC production monitoring. Hourly site irradiance satellite data is provided by The Weather Company's Cleaned Historical API for the purposes of performance ratio calculation.



Fig. 3. Oregon side-by-side bifacial site. $GCR = 0.35$, $H = 0.75$

Inspection of the site geometry showed module collector width of 2 m and row spacing of 5.65 m, and a measured GCR = 0.35. Similarly, a 1.5 m tracker hub height measurement indicates a normalized axis height $H = 0.75$. Field IV curves were taken for one bifacial module in the center of a row under three different rear albedo conditions: rear irradiance completely blocked with black cloth; natural ground cover; and high reflectance (~80%) white ground cloth. Relative to the zero rear irradiance condition, natural ground cover increased module power by 10%, and reflective ground cover increased power by 20%, under mostly sunny conditions.

C. Field Data Comparison Method

Bifacial system performance can be evaluated by comparing measured and modeled energy yield (Y_f) and performance ratio (PR) [15] for bifacial and reference monofacial systems. Measured AC electrical energy is aggregated for each site, excluding times when the site experienced inverter or tracker issues. Overall energy gain for a bifacial system is determined by comparing energy yield Y_f [kWh/kW] for both monofacial and bifacial systems [5]:

$$BG_E = 100\% \times \left(\frac{Y_{f,bifl}}{Y_{f,mono}} - 1 \right) \quad (3)$$

Although BG_E gives a value of overall system performance advantage, not all of this gain is due to a system's bifaciality. Improved low-light efficiency and better temperature coefficient can improve performance as well and will be captured in the above equation. Therefore, isolating the bifacial response requires normalization of Y_f by modeled front-side performance for both module types. Here $Y_{f,model}$ is calculated with the PVLlib single-diode model [16], [17] using inputs of hourly site irradiance data, and STC (front-side only) module parameters. If proper model coefficients including temperature coefficient are included, $Y_{f,model}$ will reflect the non-bifacial aspects of performance that differ between two module types. Eq. (3) is re-written with a correction factor based on the front-only difference expected for the two module types, which will help isolate the energy gain due to bifaciality:

$$BG_{E,bifacial} = 100\% \times \left(\frac{Y_{f,bifl} Y_{f,mono,model}}{Y_{f,mono} Y_{f,bifl,model}} - 1 \right) \quad (4)$$

The $BG_{E,bifacial}$ field-measured energy yield value is used to validate the bifacial optical models described above which model G_{rear} . Here, measured $BG_{E,bifacial}$ is compared with $BG_{E,Model}$ where

$$BG_{E,Model} = \varphi_{Pmp} \times \frac{G_{rear}}{G_{front}} (1 - \eta_{loss}) \quad (5)$$

For bifacial system performance modeling, G_{rear} and G_{front} are front and rear modeled irradiance, respectively, φ_{Pmp} is the PV module 1-sun bifaciality, (rear vs front power ratio) as defined in [18], and η_{loss} which accounts for additional bifacial loss terms such as shading loss and irradiance mismatch. Here η_{loss} is assumed to be zero, and G_{rear} is averaged across the back of the bifacial module.

IV. RESULTS

A. Model Comparison and System Optimization

The advantage of 1-axis tracking for high DNI climates is well established. Fig. 4 shows annual G_{rear}/G_{front} bifacial improvement for two modeled TMY3 climate conditions: Albuquerque, NM (high DNI), and Seattle, WA (low DNI). Both bifacial irradiance gain and front-side irradiance are reduced as tracker spacing is reduced, due to increased self-shading on the front, and reduced ground reflected irradiance on the rear surface. For a modeled albedo = 0.25 and $H = 0.75$, in Albuquerque the rear irradiance ratio ranges from $G_{rear}/G_{front} = 8\% - 9\%$. In Seattle due to increased diffuse irradiance, $G_{rear}/G_{front} = 9.5\% - 11\%$.

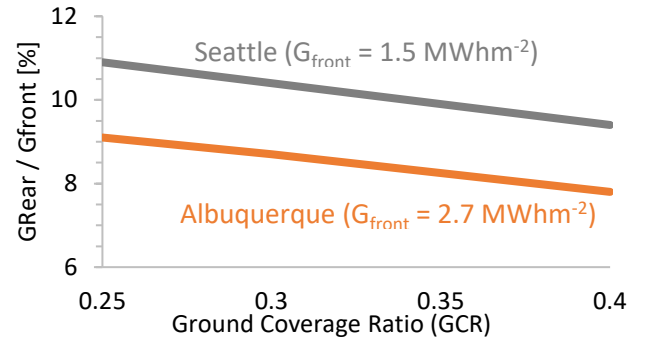


Fig. 4. G_{rear} / G_{front} irradiance modeled for two TMY3 locations. High GCR reduces rear bifacial gain (and front irradiance) due to self-shading. Assumed ground albedo: 0.25 (aged concrete).

The CF model was applied to evaluate tracker bifacial gain for many locations around the globe using satellite-based TMY irradiance data, and satellite-measured albedo values from NASA [19] (Fig. 5). The system configuration assumed was 0.35 GCR, $H = 0.75$. For some high-albedo equatorial locations, the gain from the 1-axis bifacial tracking was found to be as high as 20%, but a more typical global average value was 9%. Note that $\varphi_{Pmp} = 100\%$ and $\eta_{loss} = 0$ was assumed, which may be too optimistic for real fielded bifacial systems.

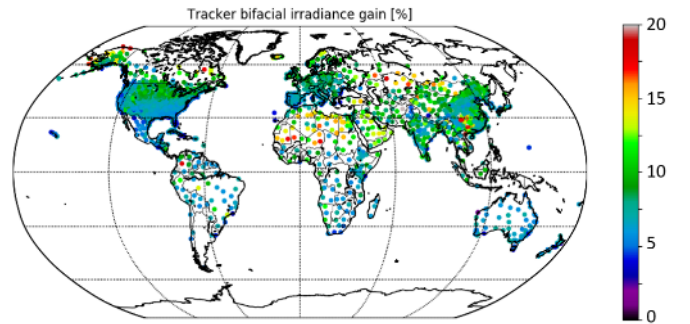


Fig. 5. Modeled G_{rear} / G_{front} [%] for 1-axis tracked systems over natural ground cover. Assumed geometry: GCR = 0.35, $H = 0.75$.

B. Sandia National Laboratory Results

Fig. 6 shows 5-minute measured and modeled G_{rear} / G_{front} for a single sunny day. It is clear that Row 1 is positioned to the east of Row 2 and therefore has a reduced G_{rear} in the morning when trackers are pointing east, and the backside has a view of the row behind. Likewise Row 2 has a reduced G_{rear} in the afternoon when trackers are pointing west and the back of the modules have an obstructed view due to the position of Row 1. Also visible is a large increase in measured BG_E for both rows during afternoon cloudy conditions. This further illustrates the increased bifacial gain that can be expected under cloudy conditions, or in climates with high diffuse irradiance fraction.

Cumulative rear vs front production is analyzed for seven months, and compared with $BG_{E, Modeled}$ using the CF model and on-site measure irradiance data. The cumulative measured BG_E shown in Fig. 7 is 11%, with monthly variation between 10-14.9%. The monthly $BG_{E, Modeled}$ varies little from month to month, with cumulative average = 12.3%. Measured values in May show anomalously large BG_E , potentially due to tracker misalignment reducing G_{front} during this month.

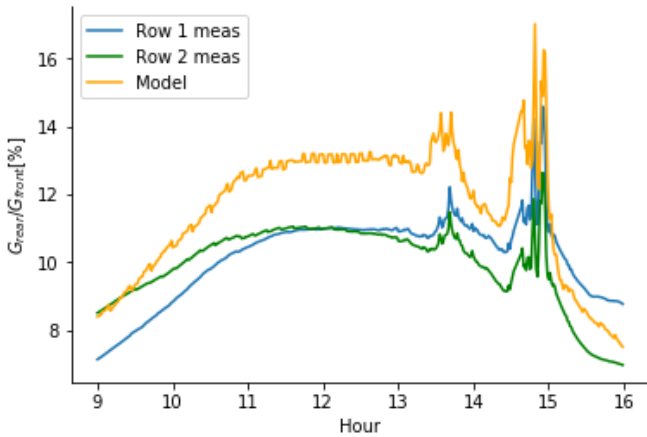


Fig. 6. Measured and modeled rear irradiance gain G_{rear} / G_{front} for March 30, 2017.

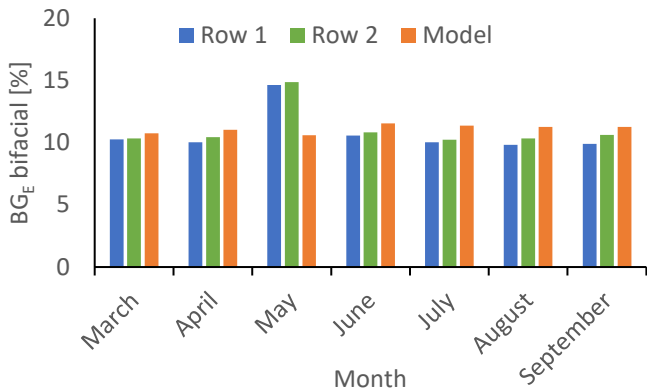


Fig. 7. CF model comparison vs SNL tracking systems from March to September. Anomalous large BG_E in May could be due to tracker misalignment.

C. Eastern Oregon Data

AC energy yield data were collected for the side-by-side bifacial and monofacial installations. Performance Ratio (PR) values range from 0.63 to 0.90 for the two systems, with a cumulative average of 0.738 for the monofacial, and 0.807 for the bifacial systems. Although field IV curve measurements indicate comparable front-side capacity for the two systems, the measured PR was on average 9.4% higher for the bifacial system than for the monofacial system.

As mentioned above, system performance can be influenced by effects other than bifaciality, including temperature coefficient differences. To isolate bifacial gain, Eq. (4) is used, with expected system PR based on site temperature, irradiance, and module nameplate (front-side) parameters. These modeled PR values are 0.777 for the monofacial, and 0.795 for the bifacial systems resulting in a corrected $BG_{E, Bifacial} = 7.0\%$. This means that approximately 2.4% of the measured performance advantage of the Silfab HIT modules is due to improved front-side performance, rather than bifacial response.

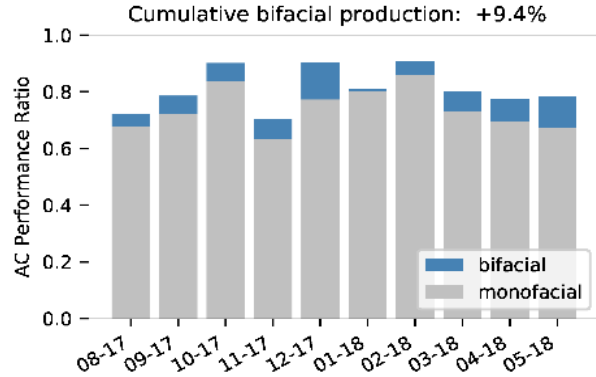


Fig. 8. Side-by-side production for two 100kW tracked systems. Bifacial PR ranged from 0.7 to 0.9 and averaged 9.4% higher than the monofacial system's PR.

Monthly $BG_{E, bifacial}$ values are shown in Fig. 8 based on measured AC energy production, as well as bifacial performance model results. Here, CF model hourly results are calculated based on site irradiance data and system geometry described in Section III. Site albedo is not known for certain, but based on tables of vegetation albedo [20], short grass typically has values of 0.15 – 0.25. Here a typical value of 0.2 is assumed. $\phi_{Pmp} = 0.95$ is also assumed, based on manufacturer datasheet estimates.

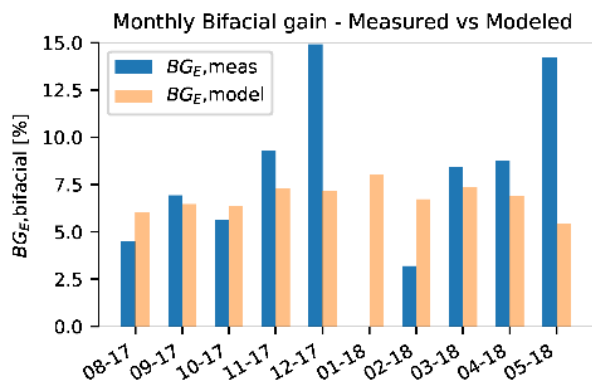


Fig. 9. Bifacial gain $BG_{E,bifacial}$ per Eq. (4) measured from AC production data, compared with CF bifacial energy gain estimates.

Fig. 9 shows that on average, $BG_{E,Model}$ is 6.7%, which is close to the measured $BG_{E,bifacial}$ of 7%. However, monthly measured values had greater variability, particularly during the snowy winter months. In particular, December, January and May showed the greatest difference from the model. December likely showed greater than expected bifacial gain because of the high albedo ground cover that boosts rear-side reflected irradiance. However, January bifacial performance was particularly bad. This underperformance was isolated to a 1-week period immediately following a heavy snow-storm where bifacial output was significantly below monofacial output. It is possible that snow was not shed from the landscape-oriented bifacial panels as quickly as from the portrait monofacial panels, which had a negative effect on the monthly comparison. The month of May is more difficult to explain and could be related to other isolated performance issues with the monofacial reference system.

D. Bifacial-Specific 1-Axis Tracker Operation and Gain

It has been previously shown for monofacial systems that optimized tracking algorithms can increase annual energy yield by up to 1% by moving the tracker off-sun closer to horizontal during cloudy conditions [21]. Gulin et al [22] showed that the optimal tilt angle can depend upon sky conditions and is not always horizontal. For bifacial tracking systems we investigate the possibility of similar optimized energy gain due to tracker alignment. For CF simulations in Albuquerque (high irradiance), energy yield improvement is albedo dependent, varying from +0.6% at albedo 0.2, to +1.1% for albedo 0.8 (Fig. 10a). This improvement is location-dependent, and locations at higher-latitudes and greater diffuse irradiance content (e.g. Seattle) can show more gain. Fig. 10b shows how the instantaneous improvement in power occurs primarily on cloudy days.

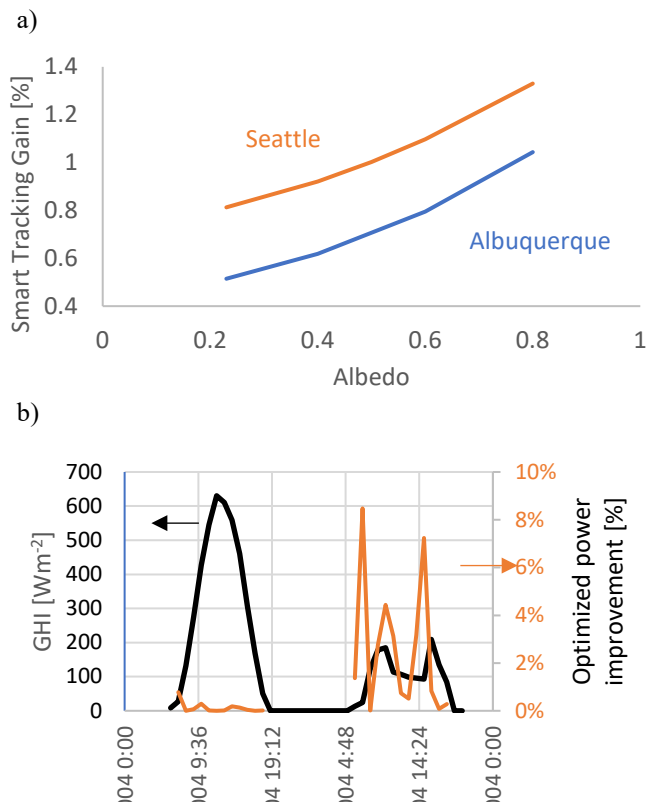


Fig. 10. a) Improvement in yearly energy capture from bifacial tracking systems for two locations, using optimized tracking. b) Power improvement for a sunny and cloudy day by operating a tracker closer to 0 tilt under cloudy conditions.

E. 1-Axis Tracker Irradiance Nonuniformity

As described in [1], the rear irradiance for tracking systems can be significantly higher at the edges of the array. For small tracking systems like the Sandia array, the effect of the finite size of the array make significant differences for models assuming infinite row extent like the CF model. Using RADIANCE, Fig. 11 investigates how many modules per row are required to meet the semi-infinite assumption at the center of the array for different clearances, finding that for any tracking height, 5 rows with 10 modules brings the G_{rear} within 5% of a semi-infinite assumption.

Even large systems will experience edge brightening at the south and north end of the row. Fig. 12 shows the average irradiance along a tracker row composed of 20 modules.

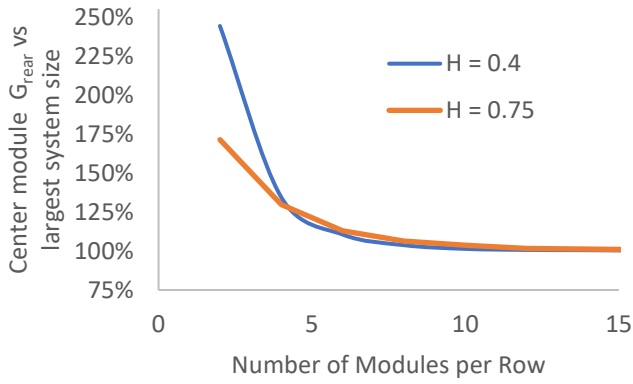


Fig. 11. BG_E for small systems is compared with a semi-infinite (20-module x 7-rows) assumption. Edge effects for different normalized clearance height $H = h/CW$ and system sizes are evaluated in Radiance. $GCR = 0.35$.

Within a distance of 5 m from the row edge, rear irradiance and BG_E is increased by 25% on the south edge, and 10% on the north edge.

The impact of shading from adjacent tracker rows has been considered here, but no additional shade losses from e.g. racking tube and frame have been considered. Some bifacial tracker designs utilize a gap between modules to limit the rear shading effect. Others mount a PV module directly onto the rack member. Radiance simulations have been conducted to assess the rear-irradiance losses from racking placed directly behind the PV module. Here, we assume a 10 cm diameter torque tube held at a distance of 10 cm – 30 cm from the module’s back. System geometry similar to that used in Fig. 12 with $H = 0.75$ is used. Hourly results are averaged over one sunny day. Results in Fig. 13 show the daily average loss in G_{rear} relative to unshaded conditions at different points along the module. Primary shading aggregates into two lobes, at a position depending on the gap between the module and tube. These shadows come from the rack blocking ground-reflected irradiance. The x separation between the two shading lobes follows the approximate dependence :

$$x_{shadow} = 2.5 \left[\left(1 - \frac{g+r}{H \cdot CW} \right)^{-1} - 1 \right] \quad (4)$$

where g is the gap between module and torque tube, and r is the torque tube radius. Other terms are defined in Eq.1 and Eq. 2. Irradiance in the center of the module seems to be increased, due in part to reflections off the top of the round torque tube. Further investigation is required to validate and to establish the overall system energy loss resulting from this shading, which will vary annually, and contribute to rear irradiance inhomogeneity.

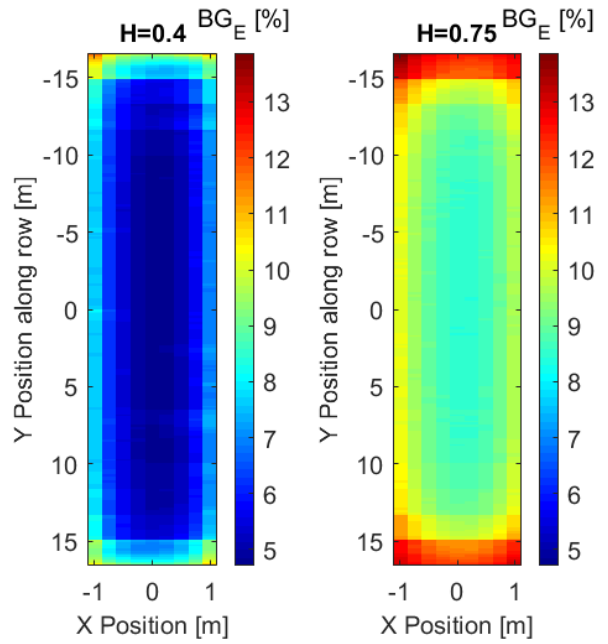
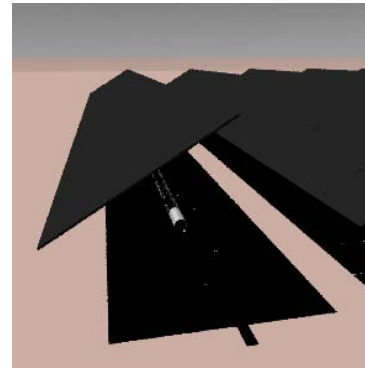


Fig. 12. BG_E is significantly higher (13.9%) at the edges of a tracker row in this 20-module x 7-row annual Radiance simulation. $GCR = 0.35$, Albuquerque climate.

a)



b)

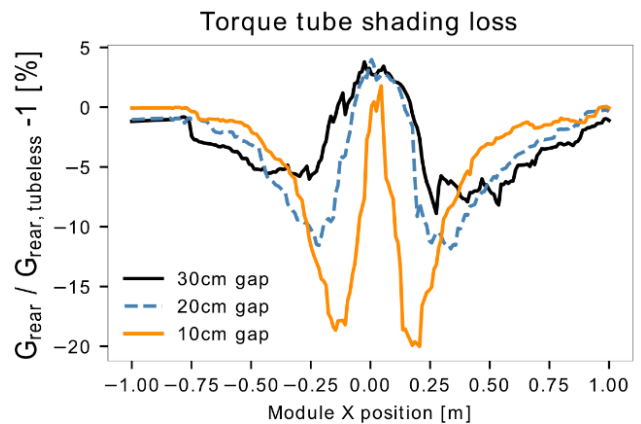


Fig. 13. a) RADIANCE image showing torque tube behind a modules row and b) G_{rear} across the module averaged over a sunny day.

V. SUMMARY

Annual energy simulations were updated to evaluate the kWh/m² boost achieved in single-axis tracking systems using bifacial modules. Measured bifacial energy gains of 7%-9% and rear irradiance gains of 11% were recorded, agreeing with modeled expectation within 1%-2% absolute, and matching global average expectation. Additional system energy gains of 0.5%-1.5% are predicted to be achieved by optimizing tracker behavior, adapting to cloudy conditions. Several sources of rear irradiance inhomogeneity were investigated, including edge brightening, and shading from center-mounted torque tubes. The latter effect was found to introduce multiple shading lobes, both at the center of the module, and also a distance from centerline depending on the gap between module and tube.

ACKNOWLEDGEMENT

This work was supported by the U.S. Department of Energy under Contract No. DE-AC36-08-GO28308 with the National Renewable Energy Laboratory (NREL). Funding provided by the U.S. Department of Energy's Office of Energy Efficiency and Renewable Energy (EERE) under Solar Energy Technologies Office (SETO) Agreement Number 30286.

REFERENCES

- [1] A. Lindsay, "Modelling of Single-Axis Tracking Gain for Bifacial PV Systems," in *Proc. 32nd European Photovoltaic Solar Energy Conference, Munich, Germany*, 2016, pp. 1610–1617.
- [2] M. Chiodetti, "Bifacial PV plants: performance model development and optimization of their configuration," M.S. Thesis, KTH Royal Institute of Technology, Stockholm, Sweden, 2015.
- [3] L. Yang, Q. H. Ye, A. Ebong, W. T. Song, G. J. Zhang, J. X. Wang, and Y. Ma, "High efficiency screen printed bifacial solar cells on monocrystalline CZ silicon," *Prog. Photovoltaics Res. Appl.*, vol. 19, no. 3, pp. 275–279, 2011.
- [4] F. Bizarri, "Innovative bifacial pv plant at la Silla Observatory in Chile," in *bifi PV Workshop 2017, Konstanz, Germany*, 2017.
- [5] J. S. Stein, D. Riley, M. Lave, C. Deline, F. Toor, and C. Hansen, "Outdoor Field Performance from Bifacial Photovoltaic Modules and Systems," in *33rd European PV Solar Energy Conference and Exhibition, Amsterdam, Netherlands*, 2017.
- [6] G. Ward, J. "The RADIANCE Lighting Simulation and Rendering System," in *Proc. 21st Annual Conference on Computer Graphics and Interactive Techniques*, 1994, pp. 459–472.
- [7] B. Marion, S. MacAlpine, C. Deline, A. Asgharzadeh, F. Toor, D. Riley, J. Stein, and C. Hansen, "A Practical Irradiance Model for Bifacial PV Modules: Preprint," in *44th IEEE Photovoltaic Specialists Conference, Washington, DC*, 2017.
- [8] C. Deline, S. MacAlpine, B. Marion, F. Toor, A. Asgharzadeh, and J. S. Stein, "Assessment of Bifacial Photovoltaic Module Power Rating Methodologies—Inside and Out," *IEEE J. Photovoltaics*, vol. 7, no. 2, pp. 575–580, 2017.
- [9] S. Ayala, C. Deline, S. Macalpine, B. Marion, J. S. Stein, and R. K. Kostuk, "Comparison of bifacial solar irradiance model predictions with field validation," *Manuscr. Submitt. Publ.*, 2018.
- [10] D. Robinson and A. Stone, "Irradiation modelling made simple: the cumulative sky approach and its applications," in *Proc. PLEA Conference, Eindhoven, Netherlands*, 2004, pp. 19–22.
- [11] R. Perez, R. Seals, and J. Michalsky, "All-weather model for sky luminance distribution—preliminary configuration and validation," *Sol. energy*, vol. 50, no. 3, pp. 235–245, 1993.
- [12] NREL, "BifacialVF," 2018. [Online]. Available: <http://github.com/NREL/bifacialvf>. [Accessed: 21-May-2018].
- [13] NREL, "Bifacial Radiance," 2018. [Online]. Available: http://github.com/NREL/bifacial_radiance. [Accessed: 21-May-2018].
- [14] W. F. Holmgren, R. W. Andrews, A. T. Lorenzo, and J. S. Stein, "PVLIB python 2015," in *2015 IEEE 42nd Photovoltaic Specialist Conference (PVSC)*, 2015, pp. 1–5.
- [15] I. E. Commission and others, "Photovoltaic system performance monitoring-guidelines for measurement, data exchange and analysis," *IEC 61724*, 1998.
- [16] W. De Soto, S. A. Klein, and W. A. Beckman, "Improvement and validation of a model for photovoltaic array performance," *Sol. Energy*, vol. 80, no. 1, pp. 78–88, 2006.
- [17] R. W. Andrews, J. S. Stein, C. Hansen, and D. Riley, "Introduction to the open source PV LIB for python Photovoltaic system modelling package," in *Photovoltaic Specialist Conference (PVSC), 2014 IEEE 40th*, 2014, pp. 170–174.
- [18] V. Fakhfour, "Photovoltaic Devices--Part 1--2: Measurement of Current-Voltage Characteristics of Bifacial Photovoltaic (PV) Devices," 2015.
- [19] C. Ichoku, "NASA Visible Earth catalog," 2018. [Online]. Available: <https://visibleearth.nasa.gov/view.php?id=60636>. [Accessed: 21-May-2018].
- [20] M. Iqbal, *An introduction to solar radiation*. Academic Press Canada, 1093.
- [21] N. A. Kelly and T. L. Gibson, "Increasing the solar photovoltaic energy capture on sunny and cloudy days," *Sol. Energy*, vol. 85, no. 1, pp. 111–125, 2011.
- [22] M. Gulin, M. Vařak, and N. Perić, "Dynamical optimal positioning of a photovoltaic panel in all weather conditions," *Appl. Energy*, vol. 108, pp. 429–438, 2013.